Optical Tristability

M. Kitano, T. Yabuzaki, and T. Ogawa

Ionosphere Research Laboratory, Kyoto University, Uji 611, Japan

It is predicted with use of a simplified model that a Fabry-Perot cavity filled with atoms with Zeeman sublevels in the ground state should exhibit optical tristability via optical pumping. For linearly polarized incident light, three stable states appear in the polarization of the transmitted light; σ_+ dominant, σ_- dominant, and linear polarizations. This optical tristability is discussed in the context of a butterfly catastrophe.

In recent years the phenomenon of optical bistability has drawn considerable interest from the aspect of practical application as optical devices[1] and also from the fundamental standpoint as a model for studying the interaction between an ensemble of atoms and a radiation field.[2] Experimentally Gibbs, McCall, and Venkatesan[3] showed that a Fabry-Perot cavity filled with sodium as a nonlinear medium exhibits optical bistability. They utilized nonlinear dispersion due to hyperfine pumping in the ground state.

In this paper we show that a Fabry-Perot cavity filled with atoms having degenerate Zeeman sublevels in the ground state exhibits optical tristability. A remarkable feature of the phenomenon is as follows. In the case of linearly polarized incident light, the polarization of the transmitted light can take a σ_+-dominant (almost right-circularly polarized) state or a σ_--dominant (almost left-circularly polarized) state in addition to a linearly polarized state. In the σ_+- (σ_--) dominant state the atomic spins in the ground state are oriented parallel (antiparallel) to the direction of the incident light beam. The spontaneous orientation comes from competitive interactions between the σ_+ and σ_- light beams in the cavity through optical pumping.

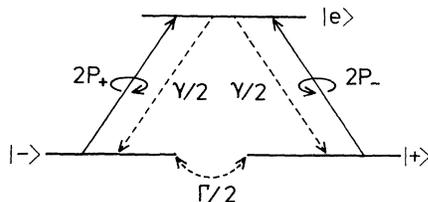We consider atoms with energy levels indicated in Fig. 1. The spin-up level $|+\rangle$ and spin-down level $|-\rangle$ in the ground state are degenerate and have equal number densities $N_+ = N_- = N/2$ in the absence of light beams, where N is the total atomic density. The optically excited levels are represented by a single level $|e\rangle$, which is possible when these levels are completely mixed by atomic collisions. In such a three-level system, the effect of optical pumping is described by the rate equations for N_+ and N_-:

$$dN_{\pm}/dt = -P_{\mp}N_{\pm} + P_{\pm}N_{\mp} - (\Gamma/2)(N_{\pm} - N_{\mp}), \qquad (1)$$

where Γ is the spin-relaxation rate, and the pumping rates $P_{\pm}$ have been assumed to be smaller than the decay rate γ of the excited state, which therefore has negligible population. The rates $P_{\pm}$ are expressed in terms of the light intensities (photon flux) $I_{\pm}$ and the absorption cross section σ by $P_{\pm} = \frac{1}{2}\sigma I_{\pm}$. For homogeneously broadened medium, the absorption cross section σ for monochromatic light of the frequency ω is given by

$$\sigma = \frac{4\pi d^2 \omega_0}{c\hbar} \frac{\gamma_{ab}}{\Delta^2 + \gamma_{ab}{}^2}, \qquad (2)$$

where d is the atomic dipole moment, γ_{ab} is the relaxation rate for optical coherence, ω_0 is the transition frequency, and $\Delta = \omega_0 - \omega$ is the atomic detuning.

The steady-state solutions of Eq. (1) are

$$N_{\pm} = \frac{\sigma I_{\pm} + \Gamma}{\sigma(I_+ + I_-) + 2\Gamma} N. \qquad (3)$$

With use of Eq. (3) the absorption coefficients $\alpha_{\pm}$ and the wave numbers $k_{\pm}$ for the σ_+ and σ_- light are

$$\alpha_{\pm} = (\sigma/2)N_{\mp}, \qquad (4)$$

$$k_{\pm} = k_0 + (\sigma/2)(\Delta/\gamma_{ab})N_{\mp}, \qquad (5)$$

where k_0 is the wave number in vacuum. For simplicity we will neglect the absorption losses by taking relatively large values of $|\Delta|$. Inclusion of absorption losses will not change the es-

FIG. 1. Simplified atomic level scheme.

sential features of our discussion. The transmission characteristics of a lossless Fabry-Perot cavity are described by the equation

$$I_{T\pm} = T^2 I_{I\pm}[1 + R^2 - 2R \cos 2k_\pm L]^{-1}, \qquad (6)$$

where $I_{I\pm}$ are the incident light intensities, $I_{T\pm}$ are the transmitted light intensities, R is the reflectivity of the mirrors, and $T = 1 - R$ is the transmissivity. The wavelengths $k_\pm$ are assumed to be constant over the entire cavity length L because standing-wave structure of the spin-polarized atoms which have relatively long relaxation time is washed out by their thermal motion. The

moving atoms are pumped by mean-field intensities in the cavity which are related to $I_{T\pm}$ by

$$I_\pm = (I_{T\pm}/T)(1 + R). \qquad (7)$$

With use of Eqs. (3) and (7) the expressions (5) for $k_\pm$ become

$$k_\pm = k_0 + 2\kappa(X_\mp + 1)/(X_+ + X_- + 2), \qquad (8)$$

where $\kappa = (\sigma/2)(\Delta/\gamma_{ab})(N/2)$ is the linear dispersion and $X_\pm = (\sigma/\Gamma)I_\pm$ are the normalized transmitted intensities. Substitution of Eq. (8) into Eq. (6) gives the following coupled nonlinear equations which relate the transmitted light intensities to those of incident ones:

$$X_\pm = T Y_\pm \left(1 + R^2 - 2R \cos\{2[k_0 + 2\kappa(X_\mp + 1)/(X_+ + X_- + 2)]L\}\right)^{-1}, \qquad (9)$$

where we introduced the normalized incident light intensities $Y_\pm = (\sigma/\Gamma)(1 + R)I_{I\pm}$.

We consider, at first, the case where the incident light is linearly polarized, namely, $Y_+ = Y_- = Y$. Equation (9) gives trivial solutions

$$X_+ = X_- = \tau Y, \qquad (10)$$

where

$$\tau = T\{1 + R^2 - 2R \cos[2(k_0 + \kappa)L]\}^{-1} \qquad (11)$$

is the transmissivity of Fabry-Perot cavity for weak-field limit $X_+, X_- \ll 1$. As for the transmitted field amplitudes and phases of both circularly polarized fields, the solutions (10) are symmetric, and the polarization of resultant transmitted light remains linear. The nonlinearity of the coupling between the two circularly polarized lights may seem to play no role in the solutions (10), but makes them unstable under some conditions.

The stability of the solutions (10) can be examined by calculating the differential gain which diverges at critical points where stable solutions become unstable under a continuous change of parameters.[1] Expanding the light intensities around the solutions (10) as $Y_\pm = Y + y_\pm$, $X_\pm = X + x_\pm$, and substituting into Eq. (9), we obtain linearized equations

$$x_+ + x_- = \tau(y_+ + y_-), \qquad (12)$$

$$x_+ - x_- = \xi_d(y_+ - y_-), \qquad (13)$$

where $\xi_d = \tau/(1 - 2\eta\tau)$ is the differential gain for the difference between both light intensities, and η is a parameter representing the strength of nonlinearity which is given by

$$\eta = (2R/T)\kappa L[X/(X + 1)] \sin[2(k_0 + \kappa)L]. \qquad (14)$$

At the critical point $\eta = \eta_{c1} = 1/2\tau$, ξ_d diverges. In the region $\eta < \eta_{c1}$, which includes the linear case $\eta = 0$, the solutions (10) are stable; hence in the region $\eta > \eta_{c1}$ they are unstable.

By using Eqs. (11) and (14), the unstable condition is written down explicitly:

$$\cos[2(k_0 + \kappa)L] + 2\kappa L \frac{X}{X + 1} \sin[2(k_0 + \kappa)L] > \frac{1 + R^2}{2R}. \qquad (15)$$

Consider the case where the inequality (15) is satisfied in the limit $X \to \infty$ by choosing adequate values of k_0, κ, L, and R. When the incident light intensities are small enough, namely, $X = \tau Y \sim 0$, the inequality (15) is not satisfied because the left-hand side is less than unity, whereas the right-hand side is greater than unity for $0 \leq R \leq 1$. Below the critical value $X_{c1} = \tau Y_{c1}$ which satisfies the equation corresponding to the inequality (15), the symmetric solutions (10) are stable. At the point $Y = Y_{c1}$ symmetry-breaking transition occurs and for $Y > Y_{c1}$ only unsymmetric solutions are stable.

To obtain the unsymmetric solutions we solved Eq. (9) numerically. In Fig. 2 we have plotted X_+ as a function of Y for $2k_0 L = -\pi/2 + 2\pi M$ (M is an integer), $2\kappa L = \pi$, $R = 0.7$. With respect to X_-, the same curves are obtained but the upper branch corresponds to the lower one for X_+, and vice versa. Increasing the incident field intensity one finds that, at the critical point Y_{c1}, X_+ jumps to the upper (lower) branch and X_- to the lower (upper) one. Above the point Y_{c1} the two stable states, i.e., σ_+-dominant and σ_--dominant states, are possible.
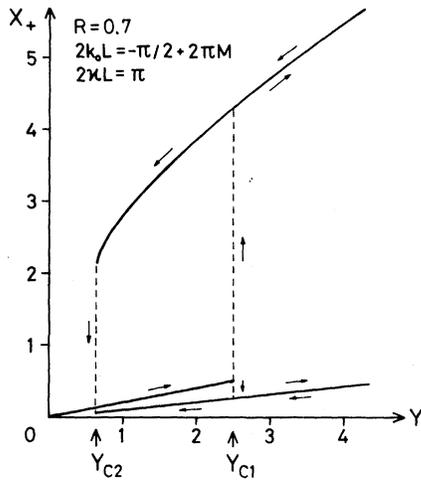
If, conversely, one decreases Y starting from

FIG. 2. Hysteresis cycles of right-circularly polarized transmitted light (X_+) in the case of linearly polarized incident light. The same curve is obtained for left-circularly polarized transmitted light (X_-) but the upper (lower) branch corresponds to the lower (upper) one for X_+. At $Y = Y_{c1}$ if X_+ jumps to the upper (lower) branch, X_- neccessarily jumps to the lower (upper) one and σ_+- (σ_--) dominant state is established.

values $Y > Y_{c1}$, one sees that, at the other critical point Y_{c2}, both X_+ and X_- jump back to the middle branch which represents the symmetric solutions (10). Thus in the region $Y_{c2} < Y < Y_{c1}$ there exists three stable solutions.

We also calculated solutions to Eq. (9) for general cases $Y_+ \neq Y_-$. In Fig. 3 we have plotted critical points on the (Y_+, Y_-) plane schematically. The single-stable, bistable, and tristable regions are indicated by the letters S, B, and T, respectively. The curve in Fig. 3 just corresponds to a section of the bifurcation set of the butterfly catastrophe[4] cut by a hyperplane $t = t_0 < 0$, $u = 0$ in the control space (t, u, v, w). The system potential for the butterfly catastrophe is represented as

$$V(x) = 1/6x^6 + 1/4tx^4 + 1/3ux^3 + 1/2vx^2 + wx, \quad (16)$$

where x is the behavior variable and corresponds to the difference $X_+ - X_-$ in our case. In Fig. 4 we have sketched the steady-state surface in the (v, w, x) space on which the derivative $\partial V/\partial x$ becomes zero, and the projection of the critical points to the (v, w) plane. The upper (lower) part of the surface corresponds to the σ_+- (σ_--) dominant state and the intermediate part corresponds to the compromised state.
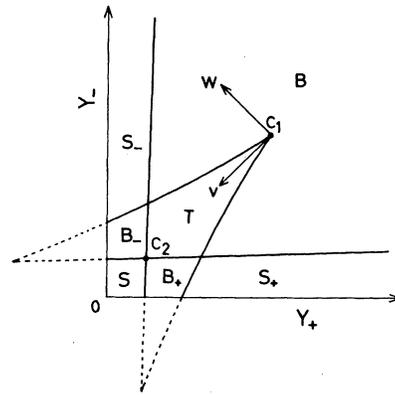
For linearly polarized incident light, the con-

FIG. 3. The plot of the critical points on (Y_+, Y_-) plane. The single-stable, bistable, and tristable regions are indicated by the letters S, B, and T, respectively. If, by changing the inputs Y_+ and Y_-, the operating point crosses the curve from region T to B or from B to S, one of the stable solutions becomes unstable and discontinuous change in outputs occurs. The curve just corresponds to the bifurcation set of the butterfly catastrophe (see Fig. 4).

trol variables move along the line $w = 0$ in Fig. 3 as the incident light intensity is varied and meet the two critical points at $Y = Y_{c1}$ and $Y = Y_{c2}$. In cases where incident light is circularly polarized, control line passes through the regions S, B_+ (B_-), and S_+ (S_-). This corresponds to the ordinary optical bistability, which has been studied in detail by Agrawal and Carmichael[5] in the context of a cusp catastrophe. In that case, the potential V is represented by a quartic polynomial including two control parameters.

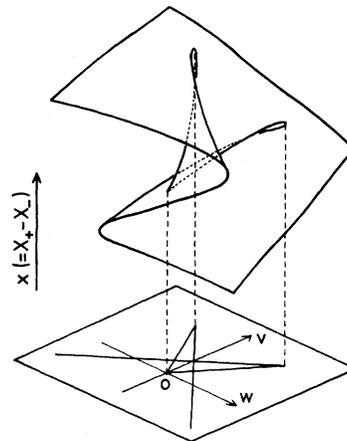Finally, we will estimate parameters for the

FIG. 4. Steady-state surface and bifurcation set for butterfly catastrophe ($t = t_0 < 0$, $u = 0$). The surface is doubly folded and is divided into three stable sheets.

experiment to realize the optical tristability in which sodium vapor is used as a dispersive medium. By filling He gas at pressure higher than 200 Torr as a buffer gas, γ_{ab} for D_1 line at 589.6 nm becomes larger than 2 GHz,[6] and we can neglect hole burning effect and hyperfine pumping especially for off-resonant light. Furthermore, the buffer gas mixes the excited hyperfine and Zeeman structure completely. Thus the situation is very close to the model which we have used in this paper. To satisfy the inequality (13), $2\kappa L$ must be of the order of unity or larger, which can be achieved by choosing $N \sim 10^{12}$ cm^{-3}, $L = 10$ cm, and $|\Delta| = 30\gamma_{ab}$. Then the absorption loss $2\alpha L$ is about 0.1 and will be neglected. The required optical power density of a cw dye laser is of the order of 10 mW/mm^2.

[1]H. M. Gibbs, S. L. McCall, A. C. Grossard, A. Passner, W. Wiegman, and T. N. C. Venkatesan, in *Laser Spectroscopy IV*, edited by H. Walther and K. W. Rothe (Springer, Berlin, 1979).

[2]R. Bonifacio and L. A. Lugiato, Phys. Rev. 18, 1129 (1978).

[3]H. M. Gibbs, S. L. McCall, and T. N. C. Venkatesan, Phys. Rev. Lett. 36, 1135 (1976).

[4]R. Thom, *Structural Stability and Morphogenesis* (Benjamin, Reading, Mass., 1975); E. C. Zeeman, Sci. Am. 234, 65 (1976).

[5]G. P. Agrawal and H. J. Carmichael, Phys. Rev. 19, 2074 (1979).

[6]D. G. McCartan and J. M. Farr, J. Phys. B 9, 985 (1976).

Instability of the Brillouin-Flow Equilibrium in Magnetically Insulated Structures

John Swegle

Sandia National Laboratories, Albuquerque, New Mexico 87185

and

Edward Ott

University of Maryland, College Park, Maryland 20742

(Received 9 October 1980)

Presented herein is a fully electromagnetic and relativistic stability analysis of the Brillouin-flow equilibrium for magnetic insulation in planar geometry. Instability of TM waves propagating in the direction of the sheared electron flow is found. This instability occurs at short wavelengths at frequencies above the cyclotron and plasma frequencies relevant to the system. It is found that relativistic effects can make the maximum instability growth rate normalized to the cyclotron frequency substantially lower than the nonrelativistic value (0.06).

PACS numbers: 52.35.Py, 52.35.Hr, 52.75.-d

In current electron and light-ion–driven inertial-confinement fusion schemes, transmission lines capable of carrying power densities of the order of 1 TW/cm^2 at electric field levels exceeding 5 MV/cm are required.[1] These stresses, far exceeding the standoff capabilities of conventional insulators, necessitate the use of a magnetic field applied perpendicularly to the electric field in a gap to prevent breakdown by electrons. Known as magnetic insulation, this method of breakdown inhibition also finds useful application in the production of intense ion beams in vacuum diodes, in relativistic magnetrons, and in multiple-stage linear accelerators for charge-neutralized ion beams. An examination of the linear stability of the magnetically insulated state is of interest in helping to determine, as a function of system parameters, the length of transmission line over which breakdown should be inhibited (or the time duration of the insulation), the quality of an ion beam which passes through an insulated electron layer, or the linear startup state of a magnetron device. In this paper, some results of the first solution of a fully relativistic and electromagnetic treatment of the stability of the magnetically insulated Brillouin-, or laminar-, flow state[2] are presented. As the name implies, electrons emitted from a cathode into this state are confined to a sheath near the cathode in which they drift laminarly along equipotentials at the local, self-consistent $\vec{E} \times \vec{B}$ drift velocity (which is sheared monotonically).

It is found that TM waves propagating along the direction of electron flow are unstable to pertur-